Analyst

Accepted Manuscript

ROYAL SOCIETY OF CHEMISTRY

www.rsc.org/analyst

Slow-Equilibration Approximation in Studying Kinetics of Protein Adsorption on Capillary Walls

Leonid T. Cherney and Sergey N. Krylov*

Department of Chemistry and Centre for Research on Biomolecular Interactions, York University, Toronto, Ontario, Canada M3J 1P3

Abstract: Adsorption of proteins on inner capillary walls affects the quality of capillary electrophoresis (CE) analyses. Coating of capillary surface with an anti-adhesive layer is typically used to suppress protein adsorption. The successful development of methods for prevention of protein adsorption requires quantitative characterization of the surface ability to adsorb and desorb a protein. It can be done by determining kinetic rate constants of adsorption, k_{ad}, and desorption, k_{des}. We have recently developed a pattern-based method for determination of k_{ad} and k_{des} for protein interaction with a capillary wall. The protein is moved through the capillary in a CE instrument by pressure and a temporal pattern of protein propagation through the detector is recorded. The experimental pattern is fitted with a numerical solution of the protein mass transfer to find k_{ad} and k_{des}. The fitting procedure is not "transparent" and can be complicated. In the present work, we obtained approximate analytical solutions of the protein mass transfer equations in the case of slow-equilibration during adsorption and desorption of the protein. These analytical solutions allow us to introduce a fitting-free parameter based method for determination of k_{ad} and k_{des}. It uses simple explicit expressions for k_{ad} and k_{des} in terms of experimental characteristics easily measured in capillaries. We tested the accuracy of the method by applying it to signals simulated with numerical solutions of protein mass-transfer equations. For the slow equilibration approximation the accuracy of k_{ad} and k_{des} was better than 12%.

Introduction

Protein adsorption in capillary electrophoresis (CE) is usually caused by negatively charged silanol groups on the inner surface of fused-silica capillaries.[1,2] Adsorption and desorption of protein molecules, A, on the capillary surface change peak shapes and thus affect the quality of protein analysis in CE-based studies.[3-6] Hence, it is highly desirable to prevent protein adsorption in CE or, at least, to take it into account in a quantitative fashion. Reducing protein-surface interaction by adjusting pH[7,8] is not possible in those analyses where keeping native protein structure is essential. Alternatively, permanent or temporary coatings can be used to cover negative surface charges and, therefore, prevent protein adsorption.[9,10] To quantitatively estimate the effectiveness of coatings and adsorption/desorption processes in CE one needs to know the kinetic rate constants of adsorption and desorption, k_{ad} and k_{des}, the equilibrium adsorption constant, $K_{ad} = k_{ad}/k_{des}$, and, sometimes, the surface concentration of total adsorption sites, N_{tot}.

Various methods have been developed to study protein and surfactant adsorption to surfaces.[11-24] These methods include ellipsometry,[12,13] reflectometry,[14-17] temperature-jump relaxation technique,[18] surface Plasmon resonance,[19] optical waveguide spectroscopy,[20] total internal reflection (TIR) fluorescence with photobleaching recovery,[21] TIR fluorescence correlation spectroscopy,[21,22] TIR fluorescence microscopy,[23] and TIR Raman spectroscopy.[24] To the best of our knowledge all studies employed flow cells with dimensions significantly larger than the diameters of capillaries used in CE. On the other hand, protein adsorption is highly dependent on the surface properties and on compounds to which the surface has been exposed previously. Thus, the optimal way for characterization of very narrow capillaries would be adsorption studies that use these capillaries as flow cells. Standard methods listed above are practically inapplicable for this purpose. Alternatively, experiments can be carried out with a plug of protein injected and driven by pressure in the absence of electric field.[6] Elution patterns of the plug with a corresponding mathematical solution for them can be used to find k_{ad}, k_{des}, K_{ad}, and N_{tot}.

Recently, we developed a pattern-based approach in which a mathematical solution is fitted into the signal generated by eluting protein at the capillary end.[25] Fitting is performed at various values of k_{ad}, k_{des}, N_{tot}, and D, where D is the diffusion coefficient of protein molecules. The best fit approximates unknown values of k_{ad}, k_{des}, and N_{tot}. In the pattern-based approach, the protein distribution in the initial plug has to be assigned arbitrarily or must be included into a set of fitting parameters. This can lead to lowered accuracy in determination of k_{ad} and k_{des} because the best fit may be achieved due to an incorrect choice of the unknown initial protein distribution rather than a correct determination of k_{ad} and k_{des}. In this work, we introduce an alternative parameter-based approach to studying protein

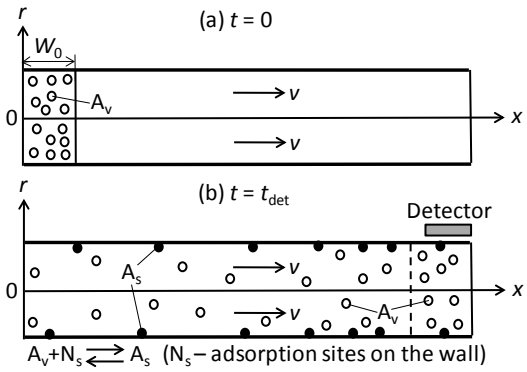

Figure 1. Experimental setup for studying adsorption and desorption of proteins in capillary flows. (a) The initial plug containing protein molecules A_v is injected into the capillary at $t = 0$. (b) The plug reaches the detector at $t = t_{det}$ (the plug rear boundary is shown by the dashed line). Protein molecules A_s adsorbed on the wall and protein molecules A_v in the volume are left in the tail behind the plug. Molecules A_v in the tail result from partial desorption of protein from the wall. The detector measures a signal that gradually decreases with an increase in time at $t > t_{det}$.

adsorption in CE. It does not require the knowledge of the protein distribution in the initial plug. In this approach an approximate mathematical solution of the protein mass transfer equations is used to obtain explicit expressions for k_{ad}, and k_{des} in terms of a few easily measured characteristics of the signal. We employ the simplest model of the reversible protein adsorption since the main purpose of this work is to develop an effective parameter-based method for estimation of protein adsorption in CE rather than to study different adsorption mechanisms.

Results and discussion

One-dimensional equations of protein mass transfer in the presence of adsorption and desorption of protein. We consider a long and narrow capillary that is coaxial with the x coordinate (**Fig. 1**). A solution containing protein A_v ("v" designates volume and "s" surface) is injected at time $t = 0$ as a short plug of length W_0. The buffer outside the plug does not contain the protein. The pressure difference is applied at the capillary ends in the absence of the electric voltage. As a result the velocity profile is parabolic with velocity vanishing at the capillary wall.[25] We assume that possible conformational changes in the adsorbed protein require much longer time than the elution time.[12,13,16] As a result, we neglect irreversible adsorption processes that can be associated with such conformational changes.[12,13,16,17,19-21] Special methods should be used in the analysis of the irreversible adsorption.[26-29] Thus, we assume that a reversible binary reaction of adsorption-desorption (1) takes place at the capillary wall

$$A_v + N_s \underset{k_{des}}{\overset{k_{ad}}{\rightleftarrows}} A_s, \quad K_{ad} \equiv k_{ad} / k_{des} \qquad (1)$$

were A_v, N_s, and A_s denote free protein molecules in the volume, free adsorption sites on the surface, and protein molecules bound to the surface, respectively. The volume concentration of A_v and the surface concentrations of N_s and A_s are denoted as A_v, N_s, and A_s, respectively.

In general, mass transfer of A_v in the presence of reaction (1) is described by a two-dimensional time-dependent differential equation since the protein volume concentration, A_v, depends on axial and radial coordinates x and r, respectively, and also on time t. However, such equation for $A_v(x, r, t)$ can be reduced to a one-dimensional time-dependent differential equation if the inner radius of capillary R and the capillary length L satisfy condition $L >> \mathrm{Pe}R$.[30-32] Here $\mathrm{Pe} = vR/D$ is the Peclet number, v is the average (across the capillary) value of the buffer velocity, and D is the diffusion coefficient of A_v. In this case, one can assume that a relative variation of protein concentration across the capillary is small. This fact allows one to use the averaging (across the capillary) procedure and Taylor's approach to describe average parameters of dispersions in narrow capillaries.[30-32] As a result, the following one-dimensional time-dependent differential equations for mass transfer can be derived[25]

$$\left(\partial_t + v\partial_x\right)A = D_T\partial_x^2 A - \frac{2}{R}\left(k_{ad}A\left(N_{tot} - A_s\right) - k_{des}A_s\right) \qquad (2)$$

$$\partial_t A_s = k_{ad}A\left(N_{tot} - A_s\right) - k_{des}A_s, \quad D_T = D\left(1 + \frac{v^2R^2}{48D^2}\right) \qquad (3)$$

Here, ∂_x and ∂_t are partial derivations by spatial coordinate x and by time t, respectively; A is the average value of the protein volume concentration, A_v, calculated across the capillary; N_{tot} is the total concentration of occupied and free active sites on the surface; D_T is the effective longitudinal diffusion coefficient determined by Taylor's expression.[30-32]. In equation (3) for A_s, we neglected the surface diffusion that is usually very small.[25]

Boundary conditions for a plug injected at the capillary inlet ($x = 0$) can be formulated as follows

$$A(t) = A_0, \quad 0 \le t \le t_0 = W_0/v; \quad A(t) = 0, \quad t > t_0 \qquad (4)$$

where W_0 is the injected plug length. Equation (2) is the second order equation and, therefore, requires one more boundary condition (in addition to relations (4)). As the second boundary condition for equation (2) we used the no-

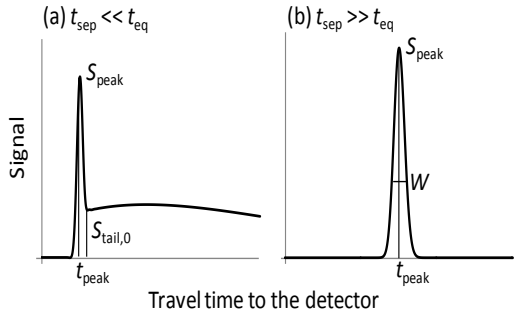

Figure 2. Two types of signal from protein in the presence of adsorption and desorption at the capillary wall: (a) a peak with a long tail behind it at slow equilibration, (b) one symmetrical peak at fast equilibration. Signals in the peak maximum and in the tail beginning are denoted by S_{peak} and $S_{tail,0}$, respectively. The time of the peak maximum, t_{peak}, and the peak width, W, are also shown. Characteristic separation and relaxation times are defined by relations (9). A value of t_{det} in Fig. 1 can be approximately defined as t_{peak}.

flux condition at the capillary outlet (i.e., $D_T\partial A/\partial x = 0$ at $x = L$). This condition is a part of Danckwerts boundary conditions.[33] Relations (4) can be also derived from Danckwerts boundary conditions taking into account that in our case the diffusion term in these conditions is small in comparison with the convective term since usually $D_T/(vW_0) << 1$. For example, $D_T/(vW_0) \sim 5 \times 10^{-3}$ for values $v = 0.02$ cm/s, $W_0 = 0.2$ cm, and $D_T = 1.72 \times 10^{-5}$ cm^2/s used in a test of applicability of the slow-equilibration approximation carried out below. Finally, initial conditions for A and A_s express the absence of protein in the initial buffer:

$$A(x) = 0, \quad A_s(x) = 0, \quad 0 < x < L, \quad t = 0 \tag{5}$$

Here, the origin of the x axis coincides with the capillary inlet.

Similarity with bimolecular reactions and relation to experimental data. Since inequality $A_s << N_{tot}$ usually holds for protein adsorption in CE,[25] the subtrahend A_s can be neglected in expression $(N_{tot} - A_s)$ that appears in equations (2) and (3). After that these equations can be rewritten in the form

$$\left(\partial_t + v\partial_x\right)A = D_T\partial_x^2 A - k_{ad}AB + k_{des}C \tag{6}$$

$$\partial_t C = k_{ad}AB - k_{des}C, \quad B = \frac{2N_{tot}}{R} = const, \quad C = \frac{2A_s}{R} \tag{7}$$

Equations (6) and (7) are identical to equations of mass transfer for bimolecular reactions in CE[34-37]

$$A + B \underset{k_{off}}{\overset{k_{on}}{\rightleftarrows}} C, \quad k_{on} = k_{ad}, \quad k_{off} = k_{des} \tag{8}$$

if B and C are the volume concentrations of B and C, respectively, and the travel velocity of C is zero (diffusion of C is assumed to be negligible). As a result, characteristic adsorption/desorption time and separation time can be defined similar to those for bimolecular reactions in CE:[36,37]

$$t_{eq} = \frac{1}{Bk_{ad} + k_{des}} = \left(\frac{2N_{tot}k_{ad}}{R} + k_{des}\right)^{-1}, \quad t_{sep} = \frac{W_0}{v} \tag{9}$$

Here, t_{eq} is the equilibration time showing how fast equilibration between adsorption and desorption of protein molecules is achieved in the capillary, t_{sep} is the separation time describing how fast protein molecules adsorbed from the plug are separated from the moving plug (i.e. are transferred to the tail). Such separation results from the plug movement that leads to adsorbed protein molecules being left behind the plug. A slow-equilibration approximation assumes that $t_{sep} << t_{eq}$. A typical value of t_{sep} in CE can be estimated as 10 s.[35] For example, in very narrow capillaries with $R = 10^{-3}$ cm, we have $v = 0.02$ cm/s, $W_0 = 0.2$ cm, and $t_{sep} = W_0/v = 10$ s. As a result, the slow-equilibration approximation can be used if $t_{eq} >> 10$ s. Given expression (9) for t_{eq} we obtain that this condition leads to simple requirements for k_{ad} and k_{des}: $k_{ad} << R/(2t_{sep}N_{tot}) \sim 25$ mM^{-1}s^{-1}, $k_{des} << 0.1$ s^{-1}. Here, we used the following estimates: $R \sim 10^{-3}$ cm and $N_{tot} \sim 2 \times 10^{-12}$ mol/cm^2.[25] Thus, the slow-equilibration approximation covers a wide range of k_{ad} and k_{des} values.

Experimental data in a form of temporal propagation pattern (e.g. electropherogram or chromatogram) operate with signals $S(t)$ that are usually proportional to the linear concentrations of detected compounds (i.e. to their amounts per unit length of the capillary) at the point where a detector is placed. In our case the total signal, S_{tot}, equals to a sum of signals S and S_s that can arise from protein molecules present in the volume and adsorbed on the surface, respectively,

$$S = S_v + S_s, \quad S_v = \pi g_v R^2 A, \quad S_s = 2\pi g_s R A_s \tag{10}$$

Here, g_v and g_s are constant coefficients that are defined by a detection method used. In the case of fluorescence detection, they can be expressed as follows:[37]

$$g_v = \frac{Q}{\chi}, \quad g_s = \frac{Q_s}{\chi_s} \tag{11}$$

where Q and Q_s are absolute quantum yields of A and A_s, respectively, χ and χ_s are proportionality coefficients. Parameters Q, Q_s, χ, and χ_s depend on the fluorophore and detector used for sensing A and A_s.[38,39]

Although mass transfer is described by the same equations (6) and (7) for both adsorption/desorption and bimolecular reactions, solutions of equations (6) and (7) can behave quite differently in these two cases. This can be caused by the difference in the initial plug composition. In the case of adsorption/desorption process, the adsorbed protein A_s is absent in the initial plug and, therefore, $C = 2A_s/R = 0$ in the plug at $t = 0$. In contrast, for bimolecular reactions, the complex C is present (usually in equilibrium with A) in the initial plug, which leads to $C \sim A$ in the plug at $t = 0$.[34-37] As a result, at $t_{sep} << t_{eq}$ we have two prominent peaks in signals for bimolecular reactions, that correspond to unbound A and intact C present in the initial plug (assuming that A is labeled for detection).[34-37] On the contrary, there is only one well pronounced peak in signals for adsorption/desorption processes at $t_{sep} << t_{eq}$ (**Fig. 2a**). This peak corresponds to the original A contained in the initial plug (i.e. A that does not result from desorption). The absence of the second peak for adsorption-desorption process does not allow to determine k_{ad} and k_{des} at $t_{sep} << t_{eq}$ by using the slow-equilibration approximation developed for studying kinetics of bimolecular reaction.[36] Thus, we have to reconsider slow equilibration approximation specifically for the case of adsorption and desorption.

The slow-equilibration approximation for protein adsorption on capillary walls. In this case, $t_{sep} << t_{eq}$ and t_{sep} is also much smaller than characteristic times of adsorption and desorption, t_{ad} and t_{des}:

$$t_{sep} << t_{ad}, \quad t_{sep} << t_{des}, \quad t_{ad} \equiv \frac{R}{2N_{tot}k_{ad}}, \quad t_{des} \equiv \frac{1}{k_{des}} \qquad (12)$$

(t_{ad} and t_{des} are defined by two last relations in (12)). Therefore, the adsorbed protein molecules are separated from the plug much faster than they can accumulate on (or desorb from) the capillary surface being in contact with the plug. Given the absence of adsorbed protein A_s in front of the plug, A_s should be depleted in the plug except at its end were the tail begins. As a result, the term $k_{des}C = 2k_{des}A_s/R$ can be omitted in equations (6) and (7) when we applied them to the major part of the plug (i.e. except its end). After excluding this term the equations take the following form in the coordinate system $\xi = x - vt$ moving with the plug:

$$\frac{dA}{dt} = D_T\partial_\xi^2 A - k_{ad}AB, \quad \frac{dC}{dt} - v\partial_\xi C = k_{ad}AB \qquad (13)$$

Here, d/dt is the derivative calculated in the moving coordinate system (i.e. at $\xi = 0$), A approximately coincides with the concentration of original A present in the initial plug since the adsorbed protein molecules do not have enough time (due $t_{sep} << t_{eq}$) to desorb back into the plug volume. Obviously, equations (13) can be also applied at the plug end if the concentration A present in (13) is still considered as the concentration of original A. This fact allows us to derive an equation for the total amount of original A, a_{plug}, by integration the first equation (13) over the plug length:

$$\frac{da_{plug}}{dt} = -\frac{a_{plug}}{t_{ad}}, \quad a_{plug} \equiv \pi R^2 \int_{plug} A d\xi \qquad (14)$$

We also took into account the relation $Bk_{ad} = 1/t_{ad}$ (it follows from (7) and (12)) and the fact that the original A vanishes outside the plug. In the second equation (13) the first term is much smaller than the second one and can be omitted (since $(dC/dt)/v\partial_\xi C \sim t_{sep}/t_{ad} << 1$). After that integration of the second equation (13) over the plug length gives the following value of C at $\xi = 0$ (we denote it by C_0):

$$C_0 = \frac{a_{plug}}{\pi R^2 v t_{ad}}, \quad C_0 \equiv \left(\frac{2A_{s,tail}}{R}\right)_{\xi = x - vt = 0} \qquad (15)$$

Here, $A_{s,tail}$ is the surface concentration of A_s in the tail. The value C_0 is determined by the concentration of A_s immediately behind the plug (i.e. in the beginning of the tail). Solving the first equation (14) and substituting the obtained expression for a_{plug} into equation (15) we have

$$a_{plug}(t) = a^0_{plug}\exp\left(-\frac{t}{t_{ad}}\right), \quad C_0(t) = \frac{a^0_{plug}}{\pi R^2 v t_{ad}}\exp\left(-\frac{t}{t_{ad}}\right) \qquad (16)$$

Obviously, the presence of A in the tail results from the desorption of A_s from the capillary wall behind the plug. To determine concentrations A_{tail} and $A_{s,tail}$ of A and A_s behind the plug one should solve system of partial differential equations (6) and (7) in the tail (i.e. at $0 < x < vt$) using the second relation (16) as a boundary condition at the beginning of tail (i.e. at the moving boundary $x = vt$). However, a value of A_{tail} at $x = vt$ can be determined from the ordinary differential equation. The latter is obtained by transforming equation (6) to the coordinate system $\xi = x - vt$ moving with the plug and by omitting the diffusion term in (6). This term is relatively small in the tail (at $D_T/vL << 1$) but can be important in the plug (since we can have $D_T/vW_0 \sim 1$ due to $W_0 << L$) causing the plug widening during its moving through the capillary. As a result, we have the following simple equation determining A_{tail} in the tail beginning

$$\frac{dA_{\text{tail}}}{dt} = -\frac{A_{\text{tail}}}{t_{\text{ad}}} + \frac{C_0(t)}{t_{\text{des}}}, \quad \xi = x - vt = 0 \qquad (17)$$

where we take into account the definition of C_0 according to the second relation (15). Substituting expression (16) for C_0 into relation (17) and solving the obtained equation we finally find the value of A_{tail} at $\xi = 0$ (it is denoted by $A_{\text{tail},0}$)

$$A_{\text{tail},0}(t) = \frac{t a_{\text{plug}}(t)}{\pi R^2 v t_{\text{ad}} t_{\text{des}}}, \quad A_{\text{tail},0} \equiv \left(A_{\text{tail}}\right)_{\xi = x - vt = 0} \qquad (18)$$

Here function $a_{\text{plug}}(t)$ is determined by the first relation (16) and the initial condition $A_{\text{tail},0}(0) = 0$ was used. Expressions (16) and (18) allow one to find t_{ad} and t_{des} if values of a_{plug} and $A_{\text{tail},0}$ are experimentally obtained at some time t. After that k_{ad} and k_{des} can be easily calculated using definitions (12) for t_{ad} and t_{des}. If the concentration of adsorption sites at the capillary surface, N_{tot}, is unknown a combination $k_{\text{ad}}N_{\text{tot}}$ can still be found along with k_{des}. It is often enough since adsorption is actually characterized by the product $k_{\text{ad}}N_{\text{tot}}$ if $A_s << N_{\text{tot}}$.

Determination of k_{ad} and k_{des} in the slow equilibration approximation. Using general expressions (10) for signals and definitions for $a_{\text{plug}}(t)$ and $A_{\text{tail},0}$ (i.e. the second relations in (14) and (18)) we can relate these characteristics to the total signal:

$$a_{\text{plug}} = \frac{1}{g_{\text{v}}} \int_{\text{plug}} S_{\text{v}} d\xi = \frac{v}{g_{\text{v}}} \int_{\text{plug}} S_{\text{v}} dt = \frac{v\sigma_{\text{peak}}}{g_{\text{v}}} \qquad (19)$$

$$A_{\text{tail},0} = \frac{\left(S_{\text{tail}} - S_{\text{s,tail}}\right)_{\xi=0}}{\pi R^2 g_{\text{v}}} = \frac{\left(S_{\text{tail}}\right)_{\xi=0}}{\pi R^2 g_{\text{v}}} - \frac{2g_{\text{s}}\left(A_{\text{s,tail}}\right)_{\xi=0}}{g_{\text{v}} R} \qquad (20)$$

Here, σ_{peak} is the area of the peak in the total signal $S(t)$ that corresponds to the plug of original protein, the subscript $\xi = 0$
indicates that the corresponding characteristics are determined at the beginning of the tail. While deriving relation (19) we also take into account that A_s is depleted in the plug and, therefore, the corresponding signal S_s can be neglected in calculation of σ_{peak}. In relation (20) the concentration $(A_{\text{s,tail}})_{\xi=0}$ can be also expressed in term of σ_{peak} using equations (15) and (19). As a result, we obtain the following relation between $A_{\text{tail},0}$ and experimentally measured characteristics $(S_{\text{tail}})_{\xi=0}$ and σ_{peak}:

$$A_{\text{tail},0} = \frac{1}{\pi R^2 g_{\text{v}}}\left(S_{\text{tail},0} - \frac{g_{\text{s}}\sigma_{\text{peak}}}{g_{\text{v}} t_{\text{ad}}}\right), \quad S_{\text{tail},0} \equiv \left(S_{\text{tail}}\right)_{\xi=0} \qquad (21)$$

Equations (16), (18), (19), and (21) allow us to find t_{ad} and t_{des} if signals σ_{peak} and $S_{\text{tail},0}$ are measured and a^0_{plug} is known. The latter condition can be overcome by measuring σ_{peak} at two different positions of detector at $x = L_1$ and L_2. Indeed, dividing the first relation (16) written down at $t = t_1 = L_1/v$ by the same equation written down at $t = t_2 = L_2/v$ and solving the obtained equation with respect to $1/t_{\text{ad}} = 2N_{\text{tot}}k_{\text{ad}}/R$ we have

$$N_{\text{tot}}k_{\text{ad}} = \frac{R}{2(t_2 - t_1)}\ln\left(\frac{a_{\text{plug}}(t_1)}{a_{\text{plug}}(t_2)}\right) = \frac{R}{2(t_2 - t_1)}\ln\left(\frac{\sigma_{\text{peak}}(t_1)}{\sigma_{\text{peak}}(t_2)}\right) \qquad (22)$$

The last equality in relation (22) follows from expression (19) for a_{plug}. Finally, solving equation (18) (wrote down at $t = t_1 = L_1/v$) with respect to $1/t_{\text{des}} = k_{\text{des}}$ and then substituting expressions (19) and (21) for a_{plug} and $S_{\text{tail},0}$ we obtain

$$k_{\text{des}} = \frac{t_{\text{ad}} S_{\text{tail},0}(t_1) - g\sigma_{\text{peak}}(t_1)}{t_1 \sigma_{\text{peak}}(t_1)}, \quad t_1 = \frac{L_1}{v}, \quad g = \frac{g_{\text{s}}}{g_{\text{v}}} \qquad (23)$$

Similar expression for t_{des} is also valid at $t = t_2 = L_2/v$.

To determine σ_{peak} and $S_{\text{tail},0}$ from experimentally measured signals we can apply a procedure of peak areas determination developed for NECEEM.[40] Since the area σ_{peak} corresponds to the original protein, its half $\sigma_{\text{peak}}/2$ can be found by the direct measurement of the area of the front half peak.[40] The latter is determined as a signal between the peak beginning t_{start} and the peak maximum t_{peak} (these points are usually well defined in experimental data). The signal $S_{\text{tail},0}$ should be measured at the peak end that corresponds to the moment $t = 2t_{\text{peak}} - t_{\text{start}}$.[40] This point is often coincides with the local minimum in $S(t)$ that is positioned after the peak (**Fig. 2a**).

Test of applicability of the slow-equilibration approximation to determination of k_{ad} and k_{des}. To study the accuracy of expressions (22) and (23) for k_{ad} and k_{des}, we need to use signals $S(t)$ obtained for components A_v and A_s participating in reaction (1) at various known values of k_{ad} and k_{des} The best way to produce such signals is to simulate them using numerical solutions of mass transfer equations for A and A_s and corresponding expressions for signal S. We performed such calculations with COMSOL Multiphysics 4.2 commercial software (COMSOL Group, Palo Alto, CA). Our developed program allows one to change basic parameters (k_{ad}, k_{des}, v, N_{tot}, W_0, and L) and to obtain a simulated signal $S(t)$. Then the latter can be utilized to back-calculate k_{ad} and k_{des} by using expressions (22) and (23). Since the true values of k_{ad} and k_{des} are known in this case, corresponding relative errors δ_{ad} and δ_{des} in determination of k_{ad} and k_{des} are easy to determine. The relative error is defined as an absolute value of the ratio between the deviation from the true value and the true value. It worth noting that numerical solution for equations (2) and (3) is also used in the pattern-based approach to finding k_{ad} and k_{des}.[25] However, the latter requires a fitting procedure that is computatively non-transparent and much more complicated than simple explicit expressions (22) and (23). We simulated more than 60 propagation patterns of

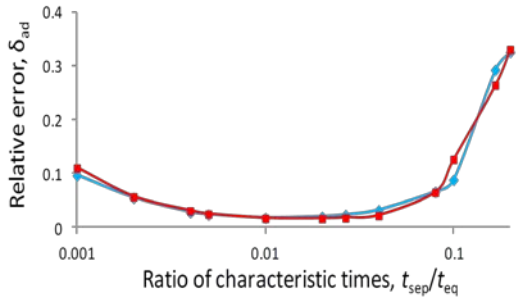

Figure 4. Relative errors in determination of k_{ad} versus the ratio of characteristic separation and equilibration times. Errors which resulted from direct measurements of the front half-peak areas of simulated signals are shown by the red line. Calculations of the peak areas based on measurements only the peak heights S_{peak} with the following use of expression (24) for σ_{peak} lead to errors depicted by the blue line.

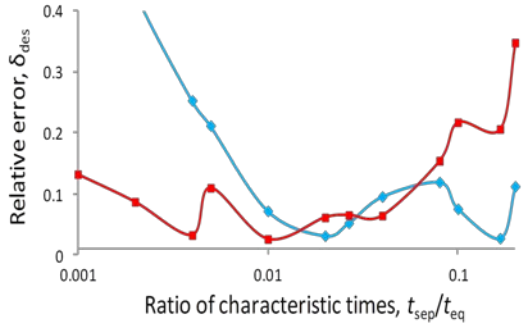

Figure 4. Relative errors in determination of k_{des} versus the ratio of characteristic separation and equilibration times. Blue and red lines correspond to $S_{tail,0}$ measured from simulated signals calculated at different distances to the detector. All points in the blue line were obtained from signals measured at the same distance $L_1 = 10$ cm. Points in the red line were obtained at different distances L_2 to the detector: $L_2 = 40$ cm (three points at the left end), $L_2 = 13$ cm (two points at the right end), and $L_2 = 20$ cm (all other points in the middle of the red line).

A_v and A_s and corresponding signals $S(t)$ mimicking experimental electropherograms. They were obtained at various values of k_{ad}, k_{des}, and N_{tot} and at four different positions of the detector. Two typical signals are shown in **Figure 2**. The values of the capillary radius, the buffer velocity and the initial plug width were $R = 10^{-3}$ cm, $v = 0.02$ cm/s, and $W_0 = 0.2$ cm, which are typical for CE experiments in narrow capillaries. We assumed, for simplicity, that $g = 1$. It should be noted that we are testing applicability of the slow-equilibration approximation that is valid in the case of $t_{sep} << t_{eq}$. Since this inequality is not affected by a value of the effective longitudinal diffusion coefficient D_T we used a fixed $D_T = 1.72 \times 10^{-5}$ cm^2/s. This value of D_T was obtained from the second relation (3) for chosen values of R and v and for a typical value of protein diffusion coefficient $D \sim 5 \times 10^{-7}$ cm^2/s. The applicability of the one-dimensional approximation (i.e., equations (2) and (3)) was tested in our previous work.[25]

Results of these "experimental" tests are presented in the two next figures. **Figure 3** shows relative errors δ_{ad} in determination of k_{ad} using expression (22) in two cases. In the first case (red line in **Fig. 3**) the peak area σ_{peak} was directly measured (as described above) using signals $S(t)$ simulated at two different distances to the detector: $L_1 = 10$ cm and $L_2 = 20$ cm. In the second case (blue line in **Fig. 3**) only the peak heights S_{peak} were measured (at the same values of L_1 and L_2). Then σ_{peak} was calculated using relation

$$\sigma(t_{peak}) = \kappa S_{peak} \sqrt{\frac{W_0^2}{4} + 4D_T t_{peak}} \qquad (24)$$

Here, the radical gives theoretical estimate of the peak width (taking into account the peak widening with time) and the coefficient κ depends on the peak shape. This coefficient disappears from expression (22) for k_{ad}.

Figure 4 shows relative errors δ_{des} in determination of k_{des} using expression (23) at different distances to the detector. All "experimental" points in the blue line (**Fig. 4**) were obtained from signals measured at the same distance $L_1 = 10$ cm. "Experimental" points in the red line (**Fig. 4**) were obtained at different distances L_2 to the detector: $L_2 = 40$ cm (three points at the left end), $L_2 = 13$ cm (two points at the right end), and $L_2 = 20$ cm (all other points in the middle of the red line). **Figure 4** demonstrates that δ_{des} can be lowered down to 12 % by increasing the distance to the detector if k_{des} is determined at the lower end of t_{sep}/t_{eq} range. In contrast, smaller values of $\delta_{des} \sim 12\%$ are achieved by decreasing the distance to the detector if k_{des} is determined at the higher end of t_{sep}/t_{eq} range. These facts can be explained as follows. The lower limit of the t_{sep}/t_{eq} ratio in **Figs 3** and **4** correspond to propagation patterns of A_v in which the tail shown in **Fig. 2a** becomes very low and difficult for observation. The latter can be partially compensated by increasing the distance to the detector. In contrast, the upper limit of the t_{sep}/t_{eq} ratio in **Figs 3** and **4** corresponds to propagation patterns of A_v in which the peak shown in **Fig. 2a** becomes too low to be clearly distinguished from the tail. To compensate this obstacle one should decrease the distance to the detector. At higher values of t_{sep}/t_{eq}, the peak corresponding to the original A_v disappears entirely. With further increase in t_{sep}/t_{eq} the single peak pattern emerges (**Fig. 2b**). The data in **Figs 3** and **4** show that the slow equilibration approximation (based on relations (22) and (23)) facilitates the determination of the rate constants k_{ad} and k_{des} and insures relative errors lower than 12% in almost entire range of the t_{sep}/t_{eq} ratio in which the peak and the tail can be identified in observed signals (i.e. at $0.001 < t_{sep}/t_{eq} < 0.1$).

Concluding Remarks

In this work, we introduced a parameter-based method for finding rate constants k_{ad} and k_{des} of adsorption and desorption of a protein on the inner capillary walls. This method works under approximations of slow equilibration

($t_{sep}/t_{eq} << 1$). The method requires measurements of the following signal characteristics: the area (or the height) of the peak corresponding to the initial protein plug and the height of the tail behind the peak. We found a new approximate analytical solution of mass-transfer equations for adsorption and desorption of proteins in capillary flows at $t_{sep}/t_{eq} << 1$. This approximate solution allows one to express k_{ad} and k_{des} in terms of easily measured characteristics of the signal. We tested the accuracy of the method by applying it to signals simulated with numerical solutions of mass-transfer equations. For the slow equilibration approximation the method's accuracy was better than 12% in the whole range of t_{sep}/t_{eq} where the peak and the tail can be identified.

ACKNOWLEDGMENT

This work was funded by the Natural Sciences and Engineering Research Council of Canada.

References

1. Chuang, I. S.; Maciel, G. E. *J. Phys. Chem. B* **1997**, *101*, 3052-3064.
2. Fan, H.-F., Li, F.; Zare, R. N.; Lin, K.-C. *Anal. Chem.* **2007,** *79*, 3654-3661.
3. Schure, M. R.; Lenhoff, A. M. *Anal. Chem.* **1993**, *65*, 3024–3037.
4. Gasš, B.; _Štědrý, M.; Kenndler, E. *Electrophoresis* **1997**, *18*, 2123–2133.
5. Towns, J. K.; Regnier, F. E. *Anal. Chem.* **1992**, *64*, 2473–2478.
6. de Jong, S.; Krylov, S. N. *Anal. Chem.* **2012**, *84*, 453–458.
7. McCormick, R. M. *Anal. Chem.* **1988**, *60*, 2322–2328.
8. Lauer, H. H.; McManigill, D. *Anal. Chem.* **1986**, *58*, 166–170.
9. Towns, J. K.; Regnier, F. E. *Anal. Chem.* **1992**, *63*, 1132–1138.
10. Regnier, F. E. *Science* **1987**, *238*, 319–323.
11. Ramsden, J. J. *Q. Rev. Biophys.* **1993**, *27*, 41-105.
12. Krisdhasima, V.; McGuire, J.; Sproull, R. *J. Colloid Interface Sci.* **1992**, *154*, 337-350.
13. Krisdhasima, V.; Vinaraphong, P.; McGuire, J. *J. Colloid Interface Sci.* **1993**, *161*, 325-334.
14. Dijt, J. C.; Cohen Stuart, M. A.; Hofman, J. E.; Fleer, G. J. *Colloids Surfaces* **1990**, *51*, 141-158.
15. Dijt, J. C.; Cohen Stuart, M. A.; Fleer, G. J. *Macromolecules* **1992**, *25*, 5416-5423.
16. Van Der Veen, M.; Cohen Stuart, M.; Norde, W. *Colloids and Surfaces B: Biointerfaces* **2007**, *54*, 136–142.
17. Furst, E. M.; Pagac, E. S.; Tilton, R. D. *Ind. Eng. Chem. Res.* **1996,** *35*, 1566-1574.
18. Ren, F. Y.; Waite, S. W.; Harris, J. M. *Anal. Chem.* **1995**, *67*, 3441-3447.
19. Silin, V.; Weetall, H.; Vanderah, D. J. *J. Colloid Interface Sci.* **1997**, *185*, 94-103.
20. Calonder, C.; Van Tassel, P. R. *Langmuir* **2001**, *17*, 4392-4395.
21. Thompson, N. L.; Burghardt, T. P.; Axelrod, D. *Biophys. J.* **1981**, *33*, 435-454.
22. Hansen, R. L.; Harris, J. M. *Anal. Chem.* **1998,** *70*, 4247-4256.
23. Kwok, K. C.; Yeung, K. M.; Cheung, N. H. *Langmuir* **2007,** *23*, 1948-1952.
24. Woods, D. A.; Petkov, J.; Bain, C. D. *J. Phys. Chem. B* **2011**, *115*, 7353–7363.
25. Cherney, L. T.; Petrov, A. P.; Krylov, S. N. *Anal. Chem.* **2015**, *87*, 1219-1225.
26. Verzola, B.; Gelfi, C.; Righetti, G. *J. Chromatogr., A* **2000**, *868*, 85–99.
27. Verzola, B.; Gelfi, C.; Righetti, G. *J. Chromatogr., A* **2000**, *874*, 293–303.
28. Castellettii, L.; Verzola, B.; Gelfi, C.; Stoyanov, A.; Righetti, G. *J. Chromatogr., A* **2000**, *894*, 281–289.
29. Tran, N. T.; Taverna, M.; Miccoli, L.; Angulo, J. F. *Electrophoresis* **2005**, *26*, 3105-3112.
30. Taylor, G. *P. Roy. Soc. Lond. A Mat.* **1954**, *A225*, 473-477.
31. Aris, R. *P. Roy. Soc. Lond. A Mat.* **1956**, *A235*, 67-77.
32. Frankel, I. & Brenner, H. *J. Fluid Mech.* **1989**, *204*, 97–119.
33. Danckwerts, P. V. *Chem. Eng. Sci.* **1953**, *2*, 1–13.
34. Okhonin, V.; Krylova, S. M.; Krylov, S. N. *Anal. Chem.* **2004**, *76*, 1507–1512.
35. Okhonin, V.; Berezovski, M. V.; Krylov, S. N. *J. Am. Chem. Soc.* **2010**, *132*, 7062-7068.
36. Cherney, L. T.; Krylov, S. N. *Anal. Chem.* **2011**, *83*, 1381-1387.
37. Cherney, L. T.; Krylov, S. N. *Analyst* **2012**, *137*, 1649-1655.
38. Chartier, A.; Georges, J.; Mermet, J. *Chem. Phys. Let.* **1990**, *171*, 347-352.
39. Parker, C.; Rees, W. *Analyst* **1960**, *85*, 587-600.
40. Cherney, L. T.; Krylov, S. N. *Anal. Chem.* **2011**, *83*, 8617-8622.

TOC Graphics